Properties of exponential many-body interatomic potentials

A. Ostapovets*, V. Paidar

Institute of Physics AS CR, v.v.i., Na Slovance 2, 182 21, Prague 8, Czech Republic

Received 10 December 2008, received in revised form 7 April 2009, accepted 20 April 2009

Abstract

A set of exponential many-body potentials of Finnis-Sinclair type was chosen to be tested for application to atomistic simulations of extended crystal defects. The selected potentials lead to stability of different lattices, fcc, hcp or bcc. The aim of this work is to test behaviour of the models based on such potentials in the cases when phase transformations can occur. In particular, the elastic constants and free surface relaxations in fcc, hcp and bcc crystals were calculated.

Key words: many-body potentials, elastic constants, multilayer surface relaxations

1. Introduction

A large variety of material properties are controlled by the phenomena, which take place on the atomic level. The knowledge of the structure of crystal lattice defects or crystallography of their motion is necessary for the studies of plastic deformation, phase transitions or fracture. An important task in these fields is a choice of description of the acting interatomic forces. Unfortunately, the determination of interatomic interactions from the first principles is not an easy task and it is combined with mathematical and calculation difficulties. Hence different approaches and simplifications are often used.

The simplest assumption is that the interaction energy can be written as a sum of pairwise contributions of the nearest neighbours to the considered atom. For example, the well-known Lennard-Jones potential belongs to this group of models. Such models can be a satisfactory approximation for certain kinds of materials such as noble gases. However, they give a description of primarily short-range forces only what is not sufficient for majority of metals. It is a well-known fact that the Cauchy relations for the models with pairwise forces are generally not satisfied in metals [1]. The next step of potential improvement was an attempt to add a term, which depends on the atomic volume [2]. However, the introduction of the atomic volume as a variable in the total energy leads to the paradox that the bulk modulus calculated by the method of long waves at constant volume differs from the value calculated for homogeneous deformation.

A progress was made by the development of embedded atom method (EAM) [3, 4] based on the density-functional and effective medium theories and Finnis-Sinclair many-body potentials [5] based on the second moment approximation to the density of states in the framework of the tight binding treatment. Both schemes give a similar form of expressions for the total energy of a system of interacting atoms although their physical justifications are different. The many-body potentials were applied to the calculations of various metal properties. For instance, the point defects, surfaces and grain boundaries have been studied in [6], the energy variation of NiAl and TiAl with structural transformation was calculated in [7]. The many-body potentials give a much better physical picture of the metal properties than the pairwise models in most cases.

Further improvement was design of the potentials, which include angular dependence of the interatomic forces. It is partially implemented in the modified EAM potentials (MEAM) [8, 9] and mainly in the bond-order potentials (BOP) [10–12]. The first approach is only a modification of EAM scheme while the second one is based on the tight binding model.

Finnis-Sinclair (FS) type many-body potential, which was proposed originally by Rosato [13] for fcc transition metals, was selected for the calculations in this work. This potential was chosen mainly for its

---

*Corresponding author: tel.: +420 2 66 052 896; fax: +420 2 86 890 277; e-mail adress: ostapov@fzu.cz

relative simplicity – it contains only five parameters. The aim of this paper is not to construct the potentials for specific materials but to find potentials with qualitatively different behaviour and to describe their properties and the trends in property changes. The potential appropriate for modelling of phase transition is in principle unstable as it describes several structures. So the main attention is paid to the question how this potential designed for fcc metals can describe the bcc structures as well. The elastic constants and properties of the simplest planar defects – free surfaces will be discussed.

2. Model

The many-body potential (1) is taken in a simple analytical form with only five parameters A, ξ, p, q, r_0 as proposed in [13],

$$U = -\sum_i (E_{\rm b}^i + E_{\rm r}^i),$$

$$E_{\rm b}^i = -\left\{\sum_j \xi^2 \exp\left[-2q\left(\frac{r_{ij}}{r_0} - 1\right)\right]\right\}^{\frac{1}{2}}, \quad (1)$$

$$E_{\rm r}^i = \sum_j A \exp\left[-p\left(\frac{r_{ij}}{r_0} - 1\right)\right].$$

In order to obtain reasonable scaling of the energy and distances, the coefficients A and ξ were fitted to the cohesive energy and lattice parameter. The parameters p and q were altered freely to change the potential property. Fitting was performed to the cohesive energy ($E_{\rm cohesive} = -2.95$ eV) and lattice parameter ($a_0 = 4.09$ Å) of silver. The fifth parameter r_0 is equal to the first neighbour separation in the fcc lattice.

Both the bonding, $E_{\rm b}^i$, and repulsive, $E_{\rm r}^i$, energy contributions for an $i^{\rm th}$ atom are cut at the distance corresponding to the $3^{\rm rd}$ neighbours of fcc lattice. Between the $3^{\rm rd}$ and $4^{\rm th}$ neighbours, the exponential expressions for $E_{\rm b}^i$ and $E_{\rm r}^i$ are replaced by the fifth order polynomials

$$P(r) = \alpha(r - r_{\rm c})^5 + \beta(r - r_{\rm c})^4 + \gamma(r - r_{\rm c})^3. \quad (2)$$

The polynomial coefficients are fitted to obtain continuity of the values and first and second derivatives at the point of line-up (the $3^{\rm rd}$ neighbour separation) and truncation to zero at the cut-off distance ($r_{\rm c}$).

Four potentials with the parameter values $p = 9$ and $q = 1$, 1.5, 2, 3, which manifest qualitatively different behaviour, were chosen for further investigation. The stability of structures, associated with such potentials, was analysed also in [14]. The most stable structures are bcc and hcp with non-ideal c/a for the potentials with $q = 1$ and 1.5, respectively, and fcc is the most stable structure for the potentials with $q = 2$ and 3.

The changes of parameters p and q alter the balance between the attractive and repulsive forces. For smaller values of q the bonding part in Eq. (1) is less steep and the contributions of the second and subsequent neighbours to the cohesive energy become larger.

Table 1. Elastic constants of fcc structure

Potential	p9q1	p9q1.5	p9q2	p9q3
C_{11} (GPa)	47.31	61.26	73.83	99.14
C_{12} (GPa)	28.37	40.63	52.59	77.96
C_{44} (GPa)	23.71	28.16	32.60	32.60
C'	9.473	10.32	10.62	10.59
Bulk modulus (GPa)	34.69	47.51	59.69	85.02
Anisotropy factor	2.50	2.73	3.07	3.08

Table 2. Elastic constants of bcc structure

Potential	p9q1	p9q1.5	p9q2	p9q3
C_{11} (GPa)	207.9	162.9	102.2	83.48
C_{12} (GPa)	90.56	80.72	71.82	86.02
C_{44} (GPa)	78.54	62.23	45.94	40.01
C'	58.69	41.09	15.20	–1.268
Bulk modulus (GPa)	129.6	108.1	81.95	85.18
Anisotropy factor	1.34	1.51	3.02	–31.55

Table 3. Elastic constants of hexagonal structure

Potential	p9q1	p9q1.5	p9q2	p9q3
C_{11} (GPa)	116.6	107.4	103.2	121.1
C_{12} (GPa)	43.6	44.7	48.2	70.3
C_{13} (GPa)	74.4	60.8	47.8	49.6
C_{33} (GPa)	261.3	189.3	119.3	120.1
C_{44} (GPa)	48.9	41.5	35.6	34.1
Bulk modulus (GPa)	79.9	74.4	67.9	83.5

3. Elastic constants

The elastic constants of fcc, bcc and hcp structures for the selected potentials are presented in Tables 1–3, respectively. Three independent elastic moduli in the cubic lattice, C_{11}, C_{12}, C_{44}, and five in the hexagonal lattice, as well as the [110] cubic shear modulus, $C' = (C_{11} - C_{12})/2$, and the value of the bulk modulus are also listed.

Table 4. Cohesive energies – E, lattice parameters – a, axial ratios – c/a and atomic volume – V of different structures. For fcc structure, the values of E, a and V are –2.95 eV, 0.409 nm and 0.01710 nm^3/atom, respectively

	Potential	p9q1	p9q1.5	p9q2	p9q3
bcc	E (eV)	–3.058	–2.964	–2.930	–2.927
	a (nm)	0.3072	0.3124	0.3180	0.3240
	V (nm^3/atom)	0.01449	0.01524	0.01608	0.01700
hcp	E (eV)	–3.018	–2.964	–2.946	–2.948
	a (nm)	0.2922	0.2920	0.2910	0.2896
	c/a	1.456	1.497	1.555	1.621
	V (nm^3/atom)	0.01574	0.01614	0.01659	0.01704

The atomic volumes that correspond to the minima on the energy-volume dependence for fcc lattices are the same for all potentials due to fitting but they are different for the other considered structures. The energies of the fcc, bcc and hexagonal structures were compared for all considered potentials. The cohesive energies, lattice parameters and atomic volumes of different structures are listed in Table 4. These values for the fcc structure are -2.95 eV, 0.409 nm and $0.01710\,\text{nm}^3$/atom, respectively. For each potential, the structure with the lowest energy is considered as stable, the others are metastable or unstable. The calculated bcc atomic volumes are smaller than the fcc or hexagonal ones.

Since the aim of this paper is to investigate how the potentials, originally developed for the fcc structure, describe the other crystal structures, it is interesting to compare the behaviour of our model with the behaviour of materials, which undergo phase transformations. As an example it is possible to take zirconium and titanium. Both of these metals undergo bcc-hcp phase transformation. The hexagonal zirconium lattice parameters $a = 0.3232$ nm and $c = 0.5148$ nm [15] correspond for the constant atomic volume to the fcc lattice parameter $a = 0.4533$ nm with the 0.3205 nm nearest neighbour separation. When the fcc nearest neighbour separation is calculated for the bcc zirconium atomic volume, 0.3179 nm, it is smaller. Hence the atomic volume of zirconium is about 2.4 % larger in the hexagonal structure than in bcc. However, in titanium the hexagonal atomic volume is about 2.8 % smaller than the bcc one.

The calculated fcc elastic constants exhibit an ascending tendency with increasing parameter q. The trends of bcc elastic constant changes are opposite. It may look as unexpected results. In fact the values of elastic constants depend on the potential derivatives at the equilibrium interatomic distances. These distances are different in the bcc and fcc lattices and they vary from one potential to another one. And so the bcc trends of elastic constant changes need not be the same as those for fcc where the lattice parameter stays constant for all the potentials due to fitting. Nevertheless, it can be concluded that the fcc lattice is more stable at higher values of q and bcc is more stable at smaller values of q [14]. This trend is similar to the trends discussed in the literature for pairwise potentials [1]. For instance, the bcc lattice is stabilized increasing the potential cut-off distance in the case of Lennard-Jones potential, i.e. including in the interaction the second and further neighbours. Moreover, the bcc lattice is unstable to the $(110)[1\bar{1}0]$ shear for the p9q3 potential since $C' < 0$.

4. Multilayer surface relaxation

The potentials were also tested by the calculations of atomic plane surface relaxation. The multilayer surface relaxation was one of important motivations for development of the many-body interatomic potentials since the pairwise potentials yield expansion of the interlayer separation between the topmost surface layers for the (100), (110) and (111) fcc surfaces what is in contradiction with the experimental data for majority of metals. We do not expect an exact description of relaxation and reconstruction processes by our simple potentials; however, the trends in behaviour of chosen potentials can be compared with those observed in experiments and calculations by other methods.

Let us consider the relaxations of (100), (110), (111) surfaces for both fcc and bcc structures, the relaxations of (112) surface in bcc are considered, too. The relaxations were performed by means of the conjugate gradient method energy minimization in the LAMMPS software package [16]. The displacements of atoms were allowed only in the direction perpendicular to the surface.

The results are presented in Table 5. The relaxations smaller than 1 % are printed by slanted fonts. First of all it is possible to see that the relaxation spread much deeper in the bcc structures than in fcc, especially for the (111) surface. The large relaxation spreads up to seven atomic layers in the case of (111) bcc surface for the p9q1 and p9q1.5 potentials, and it spreads deeper than ten layers in the case of p9q2

Table 5. Multilayer surface relaxations

Lattice	Surface	Potential	$\Delta d_{12}/d_{12}$ (%)	$\Delta d_{23}/d_{23}$ (%)	$\Delta d_{34}/d_{34}$ (%)	$\Delta d_{45}/d_{45}$ (%)	$\Delta d_{56}/d_{56}$ (%)	$\Delta d_{67}/d_{67}$ (%)
bcc	(100)	p9q1	7.77	–1.74	–1.46	*0.61*	*–0.02*	*–0.08*
bcc	(100)	p9q1.5	6.72	*–0.68*	–1.30	*0.31*	*0.06*	*–0.04*
bcc	(100)	p9q2	3.37	*–0.61*	*–0.70*	*0.07*	*0.03*	*0.0*
bcc	(100)	p9q3	–5.17	–1.08	*0.16*	*0.04*	*–0.01*	*0.0*
bcc	(110)	p9q1	2.77	–1.06	*0.13*	*–0.02*	*0.01*	*0.0*
bcc	(110)	p9q1.5	1.84	*–0.62*	*0.02*	*0.00*	*0.00*	*0.0*
bcc	(110)	p9q2	*0.39*	*–0.35*	*–0.01*	*0.01*	*0.00*	*0.0*
bcc	(110)	p9q3	–2.41	*0.04*	*0.01*	*0.00*	*0.00*	*0.0*
bcc	(111)	p9q1	9.65	–4.73	4.35	1.57	–3.94	1.15
bcc	(111)	p9q1.5	5.94	–6.62	5.81	*0.68*	–4.05	2.14
bcc	(111)	p9q2	–1.55	–9.68	8.78	–1.22	–4.30	3.52
bcc	(111)	p9q3	–16.3	–13.7	14.9	–5.34	–4.44	6.48
bcc	(112)	p9q1	2.88	2.56	–1.93	*0.27*	*0.09*	*0.17*
bcc	(112)	p9q1.5	1.84	2.06	–1.33	*–0.05*	*–0.05*	*0.04*
bcc	(112)	p9q2	–2.49	2.07	–1.60	*0.41*	*–0.26*	*0.13*
bcc	(112)	p9q3	–10.5	2.22	–2.12	1.22	*–0.61*	*0.33*
fcc	(100)	p9q1	2.10	–1.19	*–0.24*	*0.61*	*0.0*	*0.0*
fcc	(100)	p9q1.5	*0.82*	*–0.86*	*–0.01*	*0.01*	*0.0*	*0.0*
fcc	(100)	p9q2	*–0.72*	*–0.67*	*–0.02*	*0.0*	*0.0*	*0.0*
fcc	(100)	p9q3	–3.70	*–0.10*	*0.04*	*–0.01*	*0.01*	*0.0*
fcc	(110)	p9q1	3.04	*–0.16*	–1.48	*0.17*	*–0.22*	*0.08*
fcc	(110)	p9q1.5	*0.92*	*–0.22*	–1.08	*0.21*	*–0.13*	*0.06*
fcc	(110)	p9q2	–3.35	*–0.09*	*–0.94*	*0.24*	*–0.10*	*0.04*
fcc	(110)	p9q3	–9.38	1.00	*–0.79*	*0.40*	*–0.16*	*0.05*
fcc	(111)	p9q1	*0.51*	*–0.43*	*–0.05*	*0.00*	*0.00*	*0.00*
fcc	(111)	p9q1.5	*–0.32*	*–0.31*	*–0.03*	*0.00*	*0.00*	*0.00*
fcc	(111)	p9q2	–1.10	*–0.19*	*0.00*	*0.00*	*0.00*	*0.00*
fcc	(111)	p9q3	–2.57	*0.13*	*–0.01*	*0.00*	*0.00*	*0.00*

and p9q3 potentials. Such behaviour is connected with metastability of the bcc structure for the p9q2 potential and its instability for p9q3. The results of calculation for the structures, which are metastable or unstable are not meaningless in the case when the phase transformations occur. An energy barrier must be overcome in order to destroy the lattice for metastable structures. The instability of bcc structure for the p9q3 potential is associated with the softness of C' elastic constant that is often observed in real materials [17]. The results for metastable and unstable structures are considered in this paper for comparison with the stable structures.

The value of relaxation of the topmost interlayer separation varies systematically when the potentials with different parameter q, i.e. with different attractive forces, are considered. The sign of relaxation changes from positive to negative with increasing q for all the surfaces.

It is known from the experiments that majority of surface relaxations is inward. But some surfaces with anomalous behaviour exist, too. For example, Al (111) [18–21], Al (100) [22], Ni (100) [23], Ir (100), Rh (100) [24], Pt (111) [25, 26], Cu (111) [27] possess outward relaxation. Overviews of experimental and theoretical results can be found, for instance, in [28–30] for the fcc metals and in [31] for bcc. Nevertheless, the EAM calculations were not successful in description of fcc metals anomalous behaviour [29, 32], they yield inward relaxation, however, the modified EAM [9] is able to describe the multilayer surface relaxation more adequately including also anomalous expansion in fcc metals.

5. Discussion

The comparison of calculated elastic constants with the experimental data for different materials cannot be done directly since our potentials were not fitted to the elastic properties. Notice, for instance, that the bulk modulus of hexagonal zirconium markedly decreases at the phase transition to the cubic structure from 97 GPa to 60 GPa [33]. Similarly, the bulk modulus of titanium decreases about 10 % [34]. The opposite behaviour is observed for the p9q1 potential but the difference is reduced with increasing q. This behaviour correlates with the atomic volume difference between the hexagonal and bcc structures that decreases, too.

Let us compare another important characteristic that is the anisotropy factor C_{44}/C'. It is often between 2 and 3 for the fcc metals, the experimental values are 2.6 for Ni, 2.83 for Pd, 1.59 for Pt, 3.2 for Cu, 3.03 for Ag, and 2.91 for Au. These values lie close to the values obtained for our model in Table 1. The anisotropy factor for the bcc metals are 0.78 for V, 0.5 for Nb, 1.56 for Ta, 0.69 for Cr, 0.72 for Mo, and 1.01 for W. Thus the values of anisotropy factors are smaller for the bcc metals than for fcc. The same trend is observed for the potentials with the parameters, which correspond to stability region of the bcc lattice. As can be expected the anisotropy factor increases when the potential parameters approach the region of the bcc lattice instability.

The trends of multilayer relaxation can be discussed using the concept of surface roughness. It is defined in [35] as the inverse of fraction of the area occupied by the atoms of the radii equal to one half the bulk nearest neighbour distance. Namely, $\Delta d_{12}/d_{12}$,

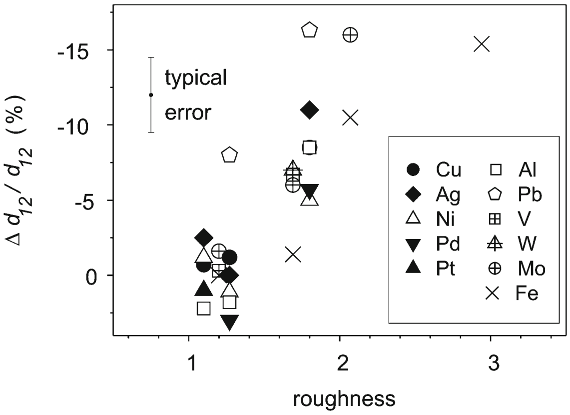

Fig. 1. Experimental values of perpendicular top layer relaxation, $\Delta d_{12}/d_{12}$, versus surface roughness for Cu (100) [37], (110) [38], (111) [39]; Ag (100) [40], (110) [41], (111) [42]; Ni (100), (110), (111) [23]; Pd (100) [43], (110) [44]; Pt (111) [25]; Al (100) [22], (110) [45], (111) [46]; Pb (100) [47], (110) [48]; Mo (100) [49], (110) [50], (112) [51]; W (100) [52]; V (100) [53], (100) [54]; Fe (100) [55], (111) [56], (112) [57]. Dimensionless surface roughness is defined in the text.

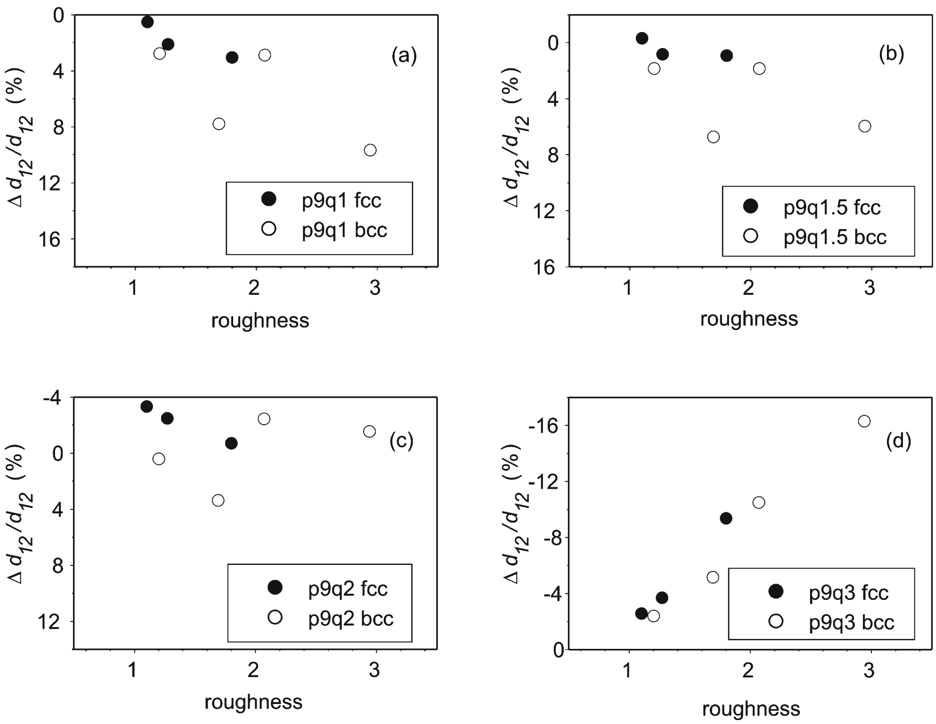

Fig. 2. Perpendicular top layer relaxation, $\Delta d_{12}/d_{12}$, versus surface roughness for p9q1 (a), p9q1.5 (b), p9q2 (c), p9q3 (d) potentials. Full circles correspond to fcc structure and empty circles to bcc. The values of roughness are 1.10 for (111) fcc, 1.27 for (100) fcc, 1.80 for (110) fcc, 1.20 for (110) bcc, 1.69 for (100) bcc, 2.07 for (112) and 2.94 for (111) bcc surfaces. Dimensionless surface roughness is defined in the text.

i.e. relative change of the first interlayer separation (in percent), can be plotted versus surface roughness. The experimental top layer relaxations rise up with increasing surface roughness (Fig. 1). Such behaviour is explained in [36] by the argument that the amount of electron redistribution is larger for more loosely packed surfaces.

The results of relaxation of the topmost interlayer distances for the many-body potentials with $p = 9$ and q from 1 to 3 are presented in Fig. 2. It is seen that the values of relaxation vary monotonously with surface roughness for the fcc lattice for all the potentials. Monotonous growth of relaxation with roughness is not observed for the bcc lattice for $q = 1$, 1.5 and 2. A trend similar to the experiments, i.e. increase of the surface relaxation with roughness (for fcc as well as bcc) is found for the p9q3 potential (Fig. 2d), but notice that the bcc structure is unstable to the $(110)[1\bar{1}0]$ shear in this case. It is necessary to note that the experimental data were obtained only for the stable structures and no structural changes were considered.

6. Conclusions

Behaviour of the models described by the many-body Finnis-Sinclair type potentials with varying parameter q of attractive interatomic forces was studied. The lattice stability is changed from fcc to bcc with decreasing q, i.e. with increasing contributions of the second and further atomic neighbours when the attractive potential part becomes stronger. The elastic constants for the fcc lattice grow up with increasing q and the trend is opposite for bcc. The loss of the bcc stability with increasing q proceeds in a physically reasonable way with decreasing C' elastic constant. The inward first layer surface relaxation is replaced by outward one for the potentials with smaller q.

Acknowledgements

The support by the COST program P19 OC149 and GAAV (project IAA100100920) is gratefully appreciated.

References

[1] CHRISTIAN, J. W.: The Theory of Transformations in Metals and Alloys. Amsterdam, Pergamon Press 2002.

[2] MAEDA, K.—VITEK, V.—SUTTON, A.: Acta Metall., *30*, 1982, p. 2001.

[3] DAW, M. S.—BASKES, M. I.: Phys. Rev. B, *29*, 1984, p. 6443.

[4] DAW, M. S.—BASKES, M. I.: Phys. Rev. Lett., *50*, 1983, p. 1285.

[5] FINNIS, M. W.—SINCLAIR, J. E.: Phil. Mag. A, *50*, 1984, p. 45.

[6] AUKLEND, G. J.—TICHY, G.—VITEK, V.—FINNIS, M. W.: Phil. Mag. A, *56*, 1987, p. 735.

[7] PAIDAR, V.—WANG, L. G.—SOB, M.—VITEK, V.: Model. Simul. Mater. Sci., *7*, 1999, p. 369.

[8] BASKES, M. I.—NELSON, J. S.—WRIGHT, A. F.: Phys. Rev. B, *40*, 1989, p. 6285.

[9] BASKES, M. I.: Phys. Rev. B, *46*, 1992, p. 2727.

[10] PETTIFOR, D. G.—OLEINIK, I. I.: Phys. Rev. B, *59*, 1998, p. 8487.

[11] AOKI, M.—NGUYEN-MANH, D.—PETTIFOR, D. G.—VITEK, V.: Prog. Mater. Sci., *52*, 2007, p. 154.

[12] MROVEC, M.—NGUYEN-MANH, D.—PETTIFOR, D. G.—VITEK, V.: Phys. Rev. B, *69*, 2004, p. 094115.

[13] ROSATO, V.—GUILLOPE, M.—LEGRAND, B.: Phil. Mag. A, *59*, 1989, p. 321.

[14] OSTAPOVETS, A.—PAIDAR, V.: Mat. Sci. Forum, *567–568*, 2007, p. 69.

[15] VILLARS, P.: Pearson's Handbook. Materials Park, ASM International 1997.

[16] PLIMPTON, S. J.: J. Comp. Phys., *117*, 1995, p. 1.

[17] SEDLAK, P.—SEINER, H.—LANDA, M.—NOVAK, V.—SITTNER, P.—MANOSA, L.: Acta Mater., *53*, 2005, p. 3643.

[18] LARAMORE, G. E.—DUKE, C. B.: Phys. Rev. B, *5*, 1972, p. 267.

[19] NIELSEN, H. B.—ADAMS, D. L.: J. Phys. C, *15*, 1982, p. 615.

[20] JONES, F.—SONDERICKER, D.—MARKUS, P. M.: J. Phys. C, *13*, 1980, p. L152.

[21] NOONAN, J. R.—DAVIS, H. L.: J. Vac. Sci. Technol. A, *8*, 1990, p. 2671.

[22] DAVIS, H. L.—HANNON, J. B.—RAY, K. B.—PLUMMER, E. W.: Phys. Rev. Lett., *68*, 1992, p. 2362.

[23] DEMUTH, J. E.—MARCUS, P. M.—JEPSEN, D. W.: Phys. Rev. B, *11*, 1975, p. 1460.

[24] OED, W.—DOTSCH, B.—HAMMER, L.—HEINZ, K.—MULLER, K.: Surf. Sci., *207*, 1988, p. 55.

[25] ADAMS, D. L.—NIELSEN, H. B.—HOVE, M. A. V.: Phys. Rev. B, *20*, 1979, p. 4789.

[26] VAN DER VEEN, J. F.—SMEENK, R. C.—TROMP, R. M.—SARIS, F. W.: Surf. Sci., *79*, 1979, p. 219.

[27] BARTOS, I.—BARBIEVI, A.—HOVE, M. A. V.—CHUNG, W. F.—CAI, Q.—ALTMAN, M. S.: Surf. Rev. Lett., *2*, 1995, p. 477.

[28] ZHANG, J.-M.—SHU, Y.—XU, K.-W.: Solid State Comm., *137*, 2006, p. 441.

[29] NING, T.—YU, Q. L.—YE, Y. Y.: Surf. Sci., *206*, 1988, p. L857.

[30] WAN, J.—FAN, Y. L.—GONG, D. W.—SHEN, S. G.—FAN, X. Q.: Model. Simul. Mater. Sci., *7*, 1999, p. 189.

[31] BREJNAK, M.—MODRAK, P.: Surf. Sci., *310*, 1994, p. L614.

[32] FOILES, S. M.—BASKES, M. I.—DAW, M. S. : Phys. Rev. B, *33*, 1986, p. 7983.

[33] LEDBETTER, H.—KIM, S.: In: Handbook of Elastic Properties of Solids, Liquids, and Glasses. Eds.: Levy, M., Bass, H. E., Stern, R. R. San Diego, Academic Press 2001, p. 97.

[34] OGI, H.—KAI, S.—LEDBETTER, H. M.—TARUMI,

R.—HIRAO, M.— TAKASHIMA, K.: Acta Mater., *52*, 2004, p. 2075.

[35] SOKOLOV, J.—JONA, F.—MARCUS, P. M.: Solid State Comm., *49*, 1984, p. 307.

[36] FINNIS, M. W.—HEINE, V.: Journal of Physics F, *4*, 1974, p. L37.

[37] LIND, D. M.—DUNNING, F. B.—WALTER, G. K.—DAVIS, H. L.: Phys. Rev. B, *35*, 1987, p. 9037.

[38] LINDGREN, S. A.—WALLDEN, L.—RUNDGREN, J.—WESTRIN, P.: Phys. Rev. B, *29*, 1984, p. 576.

[39] DAVIS, H. L.—NOONAN, J. R.: Surf. Sci., *126*, 1983, p. 245.

[40] LI, H.—QUIMN, J.—LI, Y. S.—TIAN, D.—JONA, F.—MARKUS, P. M.: Phys. Rev. B, *43*, 1991, p. 7305.

[41] NOONAN, J. R.—DAVIS, H. L.: Vacuum, *32*, 1982, p. 107.

[42] STATIRIS, P.—LU, H. L.—GUSTAFSSON, T.: Phys. Rev. Lett., *72*, 1994, p. 3547.

[43] QUINN, J.—LI, Y. S.—TIAN, D.—LI, H.—JONA, F.—MARCUS, P. M.: Phys. Rev. B, *42*, 1990, p. 11348.

[44] FEIBELMAN, P. J.: Phys. Rev. B, *46*, 1992, p. 2532.

[45] NOONAN, J. R.—DAVIS, H. L.: Phys. Rev. B*, 29*, 1984, p. 4349.

[46] JONA, F.—SONDERICKER, D.—MARCUS, P. M.: J. Phys. C, *13*, 1980, p. L155.

[47] LIN, R. F.—LI, Y. S.—JONA, F.—MARCUS, P. M.: Phys. Rev. B, *42*, 1990, p. 1150.

[48] LI, Y. S.—QUINN, J.—JONA, F.—MARCUS, P. M.: Phys. Rev. B, *40*, 1989, p. 8239.

[49] KELLY, D. G.—LIN, R. F.—HOVE, M. A. V.—SOMORJAI, G. A.: Surf. Sci., *224*, 1989, p. 97.

[50] SMITH, R. J.—HENNESSY, C.—KIM, M. W.—WHANG, C. N.—WORTHINGTON, M.—MINDGE, X.: Phys. Rev. Lett., *58*, 1987, p. 702.

[51] KOLTHOFF, D.—PFNUR, H.—FEDORUS, A. G.—KOVAL, V.—NAUMOVETS, A. G.: Surf. Sci., *439*, 1999, p. 224.

[52] FEDER, R.—KIRSCHNER, J.: Surf. Sci., *103*, 1981, p. 75.

[53] ADAMS, D. L.—NIELSEN, H. B.—ANDERSEN, J. N.: Phys. Scripta, *T4*, 1983, p. 22.

[54] ADAMS, D. L.—NIELSEN, H. B.: Surf. Sci., *116*, 1982, p. 598.

[55] LEGG, K. O.—JONA, F.—JEPSEN, D. W.—MARCUS, P. M.: J. Phys. C, *10*, 1977, p. 937.

[56] SHIH, H. D.—JONA, F.—JEPSEN, D. W.—MARCUS, P. M.: Surf. Sci., *104*, 1981, p. 39.

[57] SOKOLOV, J.—SHIH, H. D.—BARDIFY, U.—JONAF, F.—MARCUS, P. M.: J. Phys. C, 17, 1984, p. 371.